Forecasting of wind power by using a hybrid machine learning method for the Nord-Pool intraday electricity market

Atilla Altıntaş[1], Lars Davidson[1], and Ola Carlson[2]

[1]Division of Fluid Dynamics, Department of Mechanics and Maritime Sciences, Chalmers University of Technology, SE-412 96 Gothenburg, Sweden
[2]Division of Power Engineering, Department of Electrical Engineering, Chalmers University of Technology, Gothenburg, Sweden

Correspondence: Atilla Altıntaş (altintas@chalmers.se)

Abstract. The interest in trading intraday markets has been increasing due to the growth of renewable intermittent energy production. With the growing renewable energy capacity, which mostly comes from wind energy, the intraday market volume has been continuously increasing every year. In Europe, countries work with different lead times ranging from 5 to 90 minutes and trading blocks of 15 minutes. Several countries, including Sweden, use 15-minute trading blocks with 60 minutes lead time.

5   Market participants use the intraday market to optimize their position after the day-ahead market closes. Since new methods become available, such as better forecasts on short-term renewable energy power output and demand, the intraday market has become more important for energy traders in order to maximize their profit. The primary objective of this study is to enhance the intraday forecasting of wind power by improving the forecasting methods using machine learning. A hybrid approach that combines a mode decomposition method, Empirical Mode Decomposition (EMD), with Support Vector Regression (SVR),

10 is used. In addition, the forecasting with the SVR method is improved by applying a cross-validation method that tunes the parameters used. The study utilized three months (92 days) of wind turbine power data from 21 June 2017 to 20 September 2017. 80% of the data was used for training, and the remaining data were used for predictions. The results showed that combining SVR with a hybrid method that incorporates EMD predictions can lead to higher prediction accuracy. Furthermore, our results stress that parameter-tuning algorithms can improve machine-learning methods. We believe that the methods proposed in this

15 study will be beneficial for the planning of dispatchable energy generation and pricing for the intraday electricity market.

1   Introduction

The Nordic market is one of the oldest market-based electricity systems and is widely regarded as well-functioning and effective. The Nordic economy has many market structures, including a day-ahead so-called "spot" market, and an hour-ahead intraday

20 market (Hu et al., 2021).

Interest in trading intraday markets is growing as the amount of renewable intermittent energy production grows. Being balanced on the network closer to delivery time benefits both market participants and power systems by reducing the need for reserves and related costs. Furthermore, the intraday market is a critical instrument for market participants to prepare for unforeseen shifts in consumption and outages (Zavala and Messina, 2016).

25   The intraday market volume increased by 57% in 2019. This is explained by the increase in the share of variable renewable generation, mostly the increase in wind energy capacity. Since new knowledge, i.e. better renewable energy power output and demand forecasts, become available after the day-ahead market closes, market participants use the intraday market to optimize their place. In Europe, countries work with different lead times ranging from 5 to 90 minutes and trading blocks of 15 minutes. Many countries including Sweden are working with 15-minute trading blocks and 60 minutes lead time. Therefore it is crucial
30   to use a minute-scale forecast of wind power in the electricity market (Würth et al., 2019).

Wind power forecasting is an important aspect of renewable energy systems, as it helps to optimize the operation of wind farms and improve their efficiency. Various methods have been proposed for wind power forecasting, including physical methods that use atmospheric descriptions, numerical weather prediction data in statistical forecasting models (Huang and Kuo, 2018), and time-series analysis (Santamaría-Bonfil et al., 2016). The forecasting methods include autoregressive models, ARIMA
35   models, artificial neural network models, and support vector regression models Yang (2015); Tan et al. (2020); Huang et al. (2017). However, few researchers have paid attention to the forecasting problem about the wind power capacity, which plays an important role in wind power construction plans, investment, operation, and as well as energy trading plan (Yang, 2015).

Therefore, wind power forecasting is a critical aspect of renewable energy systems, and various methods have been proposed to forecast wind power output. These methods include autoregressive models, ARIMA models, artificial neural network models,
40   and also support vector regression models. Recently, hybrid methods have promised improvements in short-term wind power forecasting and uncertainty analysis (Huang et al., 2017; Liu et al., 2018). However, further research is needed to enhance the accuracy of wind power capacity forecasting.

The main objective of this study is to improve the intraday forecasting of wind power by improving the forecasting method using machine learning. A hybrid approach, which combines a mode decomposition method, Empirical Mode Decomposition
45   (EMD), with Support Vector Regression (SVR), is used (Altıntaş and Davidson, 2021; Altıntaş et al., 2023). The data used in this study are obtained from the Röbergsfjället wind farm which is located at Vansbro in Sweden and consists of eight Vestas V90-2MW horizontal axis wind turbines. The three months (92 days) of power data have been used from 21 June 2017 to 20 September 2017, 80% of the data has been used for training and the rest is used for the predictions. The data are available in seconds and averaged over 15 minutes for this study. The results imply that combining SVR with a hybrid method that
50   incorporates EMD predictions can lead to higher prediction accuracy. The planning of dispatchable energy generation and pricing for the intraday electricity market is expected to improve with higher accuracy of wind power forecasting.

2 Theory and Method

This study focuses on improving the accuracy of wind power forecasting through the application of machine learning methods. In this context, the Support Vector Regression (SVR) method was utilized as the base method for forecasting, and to improve the performance of the SVR method, the empirical mode decomposition (EMD) method was employed as a pre-processor (EMD-SVR). The forecasting results are compared to evaluate the contribution of the mode decomposition method.

In addition, a cross-validation (CV) method is applied to optimize the SVR method by tuning its parameters (SVR-CV). The forecasting accuracy of the SVR-CV method is compared with that of the SVR method.

Overall, this study aims to provide insights into how machine learning methods can be used to improve the accuracy of wind power forecasting and the potential benefits of combining multiple techniques for even better performance. A more detailed description of the methods is given below.

2.1 Support Vector Regression (SVR) Method

SVR is an algorithm for machine learning, which is a variant of Support Vector Machine (SVM). (Altıntaş et al. (2022)). SVR has widely been applied to forecasting problems. For a time-series data,

$$D = (X_i, y_i), 1 \leq i \leq N,$$

where X_i represents the ith element and y_i corresponds the target output data. The SVR function, f, is a linear function that is issued to formulate the nonlinear relation between input and output data as $f(X_i) = \omega^T \phi(X_i) + b$, where ω, b, and $\phi(X_i)$ are the weight vector, bias, and the function that maps the input vector X into a higher dimensional feature space, respectively. ω and b are obtained by solving the optimization problem:

$$min \frac{1}{2} \parallel \omega \parallel^2 + C \sum_{i=1}^{N} (\xi_i + \xi_i^*) \tag{1}$$

subject to:

$$y_i - \omega^T(\psi(x)) - b \leq \epsilon + \xi_i$$
$$\omega^T(\psi(x)) + b - y_i \leq \epsilon + \xi_i \tag{2}$$
$$\xi_i, \xi_i^* \geq 0.$$

The first term of Eq. 1 measures the flatness of the function. The parameter C balances the trade-off between the complexity of the model and its generalization ability. The cost of error is measured by the variables, ξ_i and ξ_i^*.

The final SVR function is obtained as:

$$y_i = f(X_i) = \sum_{i=1}^{N} ((\alpha_i - \alpha_i^*) K(X_i, X_j)) + b \tag{3}$$

where $K(X_i, X_j)$ is the Kernel function Qiu et al. (2017) and α_i and α_i^* are the Lagrange multipliers.

3

75   Python programming language and *scikit-learn 1.1.2* package have been used for SVR. The radial basis function (RBF) is chosen as the kernel function for the base method (SVR), then the Kernel function is written as:

$$K(X_i, X_j) = exp(-\gamma \|X_i - X_j\|^2), \tag{4}$$

where the parameter γ, defines the degree to which the effect of a single example of training reaches. In this study, the base method parameters are set to, $\gamma = 0.96$, $C = 1.0$, which balances the trade-off between the complexity of the model and its

80   generalization ability, and the maximum error, ϵ, is set to 0.03, and are used for all the predictions.

2.1.1   Tuning parameters with cross-validation

In the first part of the study, the process of finding the best parameters by trying many possible combinations of the SVR parameters was performed once only for the first simulation, and the parameters are kept fixed for the rest of the study. In the second stage, a parameter tuning application is applied, and the best combination of the parameters suggested by the cross-validation

85   method is applied in the SVR method. The parameter tuning method is applied as below:

The *GridSearchCV* function from the *scikit-learn* library was used for cross-validation in the parameter tuning process. The parameters used in the cross-validation are shown in Table 1.

Table 1. Parameter Grid for tuning Support Vector Regression

Parameters used in cross validation	
Kernel	'rbf', 'linear'
C	1, 2, 3, 4, 4.3, 5, 10, 100
Epsilon	0.01, 0.02, 0.03, 0.05, 0.1, 0.2, 0.27, 0.3, 0.5, 0.8, 1.0
Gamma	0.01, 0.1, 0.2, 0.3, 0.5, 0.7, 0.9, 0.95, 0.96, 1.0

The kernel options used in cross-validation are 'rbf' and 'linear', while the values for C, epsilon, and gamma are varied to

90   find the best combination of parameters. The values for C range from 1 to 100 with increments of 1 or specific values like 4.3, and the values for epsilon range from 0.01 to 1.0 with various increments. The values for gamma range from 0.01 to 1.0 with specific values like 0.95 and 0.96.

The linear kernel function is:

$$K(X_i, X_j) = \varphi(X_i).\varphi(X_j). \tag{5}$$

95   The next step is evaluating the combinations of the parameters for the best performance. To achieve this, *make_scorer* function of the *Scikit − learn* library has been used. A score metric value is generated according to the lower mean squared

error. Finally, the model with the best parameters which is obtained by using the *best_params_* attribute of the *GridSerachCV* has been used to fit the model using the training set data.

This parameter-tuning process is applied in the second stage of the study, and the best combination of parameters suggested
100 by the cross-validation method is used in the SVR method for each prediction.

2.2 Scale decomposition by Empirical Mode Decomposition

Empirical Mode Decomposition (EMD) is based on the concept that any data signal can be decomposed into a set of fundamental intrinsic oscillations, where the original signal is a combination of these oscillations. Each of these oscillations is referred to as an Intrinsic Mode Function (IMF), which satisfies two conditions: (1) the local extrema and zero-crossing numbers must
105 be equal or differ by at most one, and (2) the mean of the curve formed by connecting the maxima and minima should be zero Huang et al. (1998); Altıntaş et al. (2019).

To apply EMD to a continuous time series $X(t)$, an algorithm can be written as follows. Fluctuations are obtained by subtracting the time-averaged data, resulting in the time history data oscillating around zero.

1. Obtain all the local maxima and minima, see Fig. 1(a).
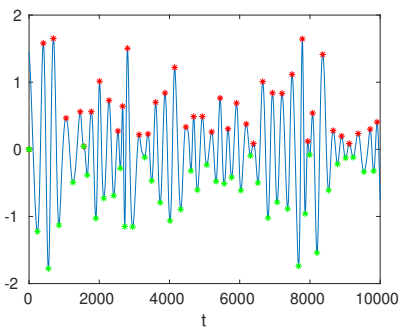
(a) All local maxima (red points), and local minima (green points).
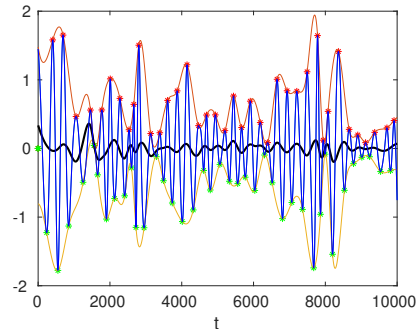
(b) Construction of the mean curve by applying a cubic spline.

Figure 1. Finding maxima, minima, and constructing a curve.

110 2. Construct an envelope curve for maxima and minima, and calculate the mean curve of these two envelope curves denoted as $m_{11}(t)$, as shown in Fig. 1(b).

3. Compute $h_{11}(t) = h_{10}(t) - m_{11}(t)$, where $h_{10}(t)$ represents the first IMF constructed from the raw data $X(t)$. The indices i and j in $h_{ij}(t)$ denote the number of the IMF in construction and the number of iterations, respectively.

4. Repeat steps (i), (ii), and (iii) recursively to obtain $h_{1k}(t) = h_{1(k-1)}(t) - m_{1k}(t)$, where k denotes the iteration number. The stopping criterion is defined as follows for $0 \le t \le T$:

$$sd_n = \sum_{t=0}^{T} \left(\frac{\left| h_{n(k-1)}(t) - h_{nk}(t) \right|^2}{h_{n(k-1)}^2(t)} \right)$$

Empirically, a number $sd_n < \epsilon$ is defined as the stopping criterion, where ϵ is a number between 0.1 and 0.3.

115

5. Once the first IMF, i.e. $h_{1k}(t)$ is found, it is subtracted from $h_{10}(t)$ to obtain $h_{20}(t)$. The process then restarts from (i) to find the second IMF.

6. Set $c_i(t) = h_{ik}(t)$, where $c_i(t)$ is the ith. IMF. The process continues until subtraction at step (v) yields monotonic or constant data (residue), indicating that all the IMFs have been obtained.

Upon applying the Empirical Mode Decomposition (EMD) process, a set of Intrinsic Mode Functions (IMFs) are obtained as a result. For instance, considering the signal $X(t)$ as depicted in Figure 2(a), which can be mathematically expressed as:

$$X(t) = 4cos(10t) + 2cos(t) + 3$$

. The resulting IMFs from the EMD process will represent the frequency components of the original signal $X(t)$. The first IMF

120 corresponds to the highest frequency component, which is $4\cos(t)$, while the second IMF is $2\cos(t)$. The residual component, also known as the residue, is represented by the constant term 3. This is illustrated in Figure 2(b).

(a) $x(t) = 4cos(10t) + 2cos(t) + 3$.
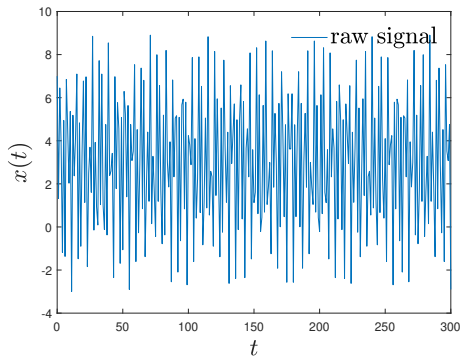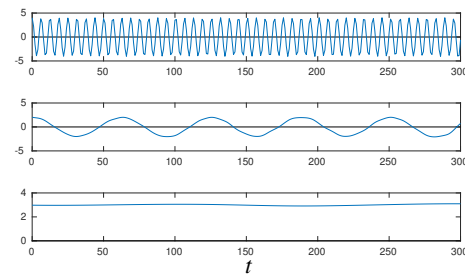
(b) IMF1 $= 4cos(10t)$, IMF2 $= 2cos(t)$, residual $= 3$.

Figure 2. EMD divides raw data into the IMFs.

3 Wind Power Data

The data are from the Röbergsfjället wind farm which is situated at Röbergskullen in the southernmost section of the Swedish municipality of Vansbro (60160 49.8"N, 14120 59.6"E)(see Fig. 3). The wind farm was constructed in 2007, with its highest

125   point being 543 meters above sea level. There are 284 meters between the wind farm's highest and lowest elevations. It consists of eight Vestas V90-2MW horizontal axis wind turbines (Abedi et al., 2021). The wind turbine that has been used for this study is highlighted with the red pin in Fig. 3(a) and also the area is highlighted in a larger map in Fig. 3(b).

The data consist of a list of records including power, hub direction, pitch angle, rotor RPM, temperature, wind direction, and wind speed for the period of 21 June 2017 to 3 February 2019. The data are recorded every second.
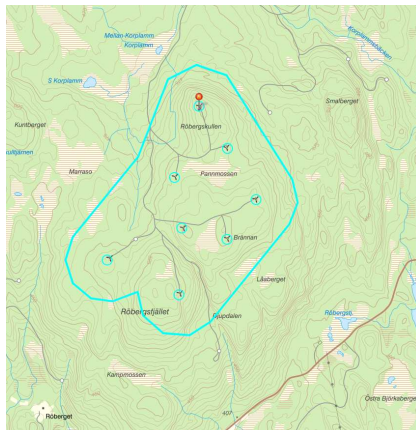
(a) Röbergsfjället wind farm. The data is from the wind turbine pointed with the red pin. The map is taken from Vindbrukskollen (see Ref. (Vin)).

(b) Location of the windfarm Röbergsfjället. The map is taken from Vindbrukskollen (see Ref. (Vin)).

Figure 3. Wind farm and turbine location.

130   The wind turbines measure the wind speed with an anemometer which is installed at a specific location on the nacelle. This anemometer is installed behind the blades and thus exposed to turbulence generated by the rotor blades. Therefore we can not trust the wind speed measured in the downstream wake area, and the wind direction is also not trusted for the same reason. Moreover, it is a pointwise measurement, however, the wind speed field that creates power is the rotor plane area which is far from homogeneous. For these reasons, we can not use wind speed from the anemometer. In this study, output power history

135   data has been used.

The three months of data were used from 21 June 2017 to 20 August 2017. Thus we try to capture seasonal wind behavior. For the same reason, the data between $11:00$ to $17:00$ have been used.

In the intraday electricity market in Sweden, trading is conducted in 15-minute intervals, with a lead time of 60 minutes. To forecast the future output power of wind farms, historical wind power data are utilized. These data are divided into time-windows

140   that are averaged over 15-minute intervals. For instance, the window $11:00-11:15$ represents the data that has been averaged over 15 minutes in the given interval. There are missing records, meaning that for some seconds the turbine has generated no power, which are excluded. To make accurate predictions, the previous four time-windows are used as input to forecast the wind power output for a time-window that is 60 minutes ahead. This approach allows for a more precise and informed prediction of the future wind power output, taking into account the historical data and the 15-minute trading blocks with a 60-minute lead

145 time used in the intraday electricity market in Sweden. An illustration of the prediction for the time-window 13:00-13:15 is illustrated in Figure 4.
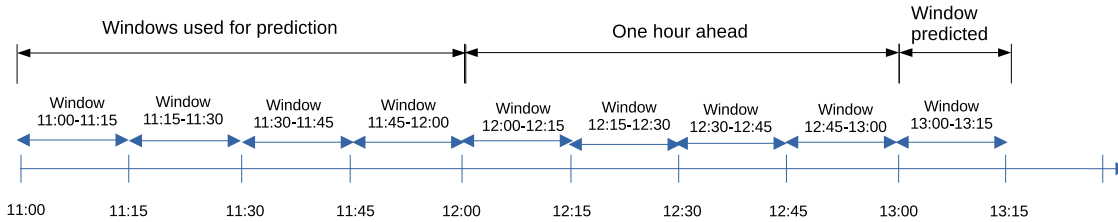
Figure 4. The power prediction for the time-window 13:00-13:15 is illustrated. The four previous time-windows have been used as an input with 60 minutes leading time, similar to the intraday market working timeline in Sweden.

4 Results

4.1 Base method, (SVR), compared to the hybrid method (EMD-SVR)

The results of applying Support Vector Regression (SVR), to forecast the future power output of wind turbine data are compared

150 with a hybrid method called EMD-SVR. The test data used for evaluation corresponds to the last 19 days, which is approximately 20% of the total 92 days of data. It should be noted that all parameters for both SVR and EMD are kept the same for all predictions.

SVR is applied using the original data, without any decomposition, as the feature. On the other hand, EMD-SVR uses Empirical Mode Decomposition (EMD) as a preprocessor to SVR, where the original data is decomposed into its Intrinsic Mode Functions (IMFs), and each IMF is used as a feature for SVR.

155 Figure 5 presents a total of 16 predictions for 15-minute averaged time-windows in the time interval of 13:00 - 17:00. The first predicted time-window is 13:00-13:15, in accordance with the intraday market timeline, as illustrated in Fig. 4. Fig. 5 provides a visual representation of the power prediction error (RMSE) for the different time-windows, and the comparison between SVR and EMD-SVR in terms of their accuracy in forecasting the future power output of the wind turbine. Table 1 displays these errors together with the mean values of the 19 days of power generation and predictions, with the best approximation provided

160 in a separate column and highlighted in red. The errors are calculated using the formula:

$$RMSE = \sqrt{\frac{\sum_{i=1}^{n}(y_i - y_i^*)}{n}}, \qquad (6)$$

where y_i, and y_i^* are i_{th} real and predicted data, respectfully.

The comparison of SVR and EMD-SVR reveals that for the time-windows 13:00 - 13:15, 13:15 - 13:30, 14:15 - 14:30, 14:45 - 15:00, and 15:15 - 15:30, EMD-SVR performs better than SVR. This indicates that in approximately 31% of the cases,

165 using the IMFs as features in EMD-SVR yields better predictions compared to using the raw data as the feature, as shown

8

in Fig.5 and Table2. Among the IMFs, IMF 1, which represents the highest frequency mode of the real data, shows better agreement with the real data in 14 out of 16 time-windows. This can be explained by the concept of mode decomposition, where high-frequency modes represent short-term changes and low-frequency modes represent long-term changes. Since this study focuses on short-term predictions for the intraday market, IMF 1 outperforms the lower frequency components.

170   The minimum and maximum errors obtained in the predictions are 6% and 16%, respectively, indicating the performance of the forecasting methods.
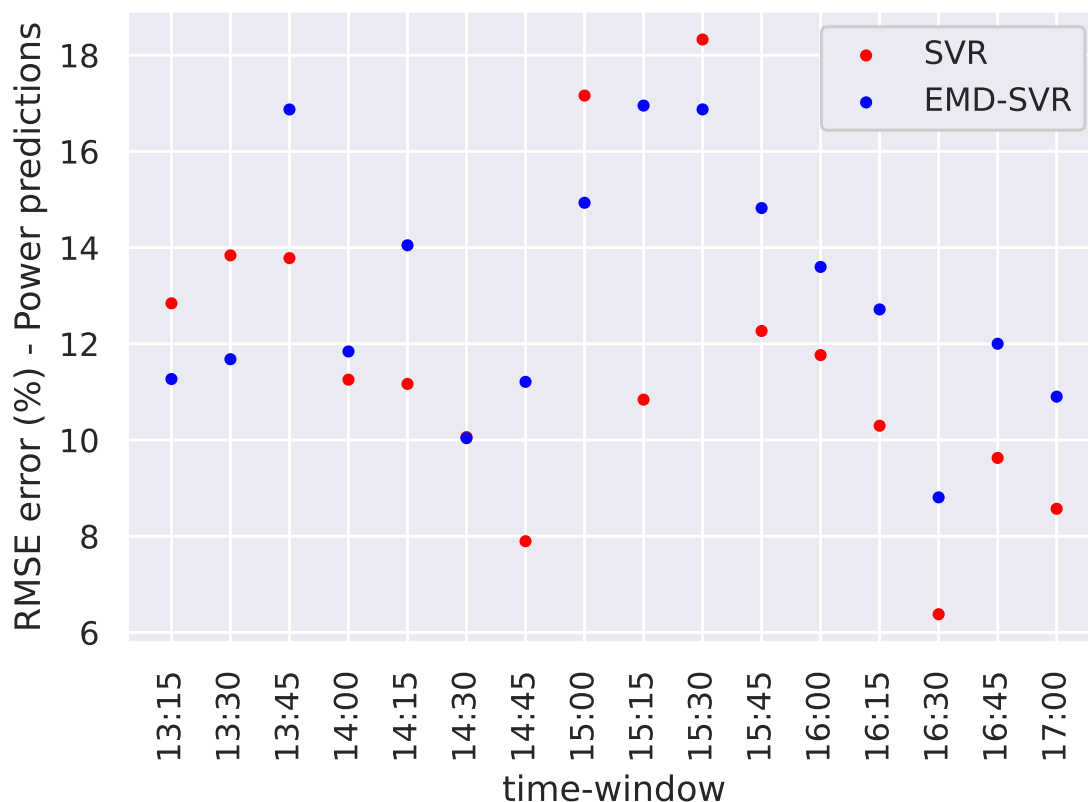
Figure 5. The power prediction error for the time-windows 13:00-13:15 to 16:45-17:00. 80% of the data has been used for the training and the rest of the data is used for the predictions that are compared with the real data. SVR compared to EMD-SVR.

Table 2. The power prediction errors for the time-windows between 13:00-17:00. RMSE = root mean square error. SVR compared to EMD-SVR.

Window	SVR compared to SVR-EMD					
	Real data	Raw prediction ()	IMF prediction	Raw prediction RMSE	IMF RMSE	Best performed IMF
13:00-13:15	436.6414	431.1161	433.7931	0.1284	0.1126	IMF 1
13:15-13:30	454.2678	437.7086	414.6955	0.1383	0.1168	IMF 1
13:30-13:45	513.9758	450.5968	424.7050	0.1378	0.1687	IMF 1
13:45-14:00	466.5867	468.1083	451.2093	0.1125	0.1184	IMF 1
14:00-14:15	463.8826	495.3884	596.7382	0.1116	0.1404	IMF 1 + 2
14:15-14:30	455.6234	539.7051	473.4623	0.1006	0.1003	IMF 1
14:30-14:45	465.4522	517.7594	419.2350	0.0789	0.1120	IMF 1
14:45-15:00	412.4164	624.0937	539.3825	0.1716	0.1493	IMF 1
15:00-15:15	419.6866	508.4634	598.2410	0.1083	0.1695	IMF 1
15:15-15:30	420.9805	582.9539	271.1095	0.1832	0.1687	IMF 1
15:30-15:45	424.9075	509.5947	343.4454	0.1226	0.1482	RESIDUAL
15:45-16:00	454.6959	486.7116	503.4796	0.1176	0.1359	IMF 1
16:00-16:15	479.6587	411.2667	459.8857	0.1029	0.1271	IMF 1
16:15-16:30	447.9367	389.1476	426.0646	0.0637	0.0880	IMF 1
16:30-16:45	491.8764	463.3234	533.6140	0.0962	0.1200	IMF 1
16:45-17:00	488.9956	426.7180	382.6640	0.0857	0.1090	IMF 1

4.2 Base method, (SVR), compared to cross-validation application (SVR-CV)

In this stage of the study, the parameters used in support vector regression (SVR) are tuned using a cross-validation method (see Section 2.1.1). The error for the predictions are presented in Fig 6, while the performance table can be found in Table 6. The best parameters obtained from the cross-validation application are displayed in a separate column. The root mean square error (RMSE) is calculated, and the differences between SVR and SVR-CV are provided in a separate column, where positive values indicate that SVR-CV provides better approximations compared to SVR. SVR-CV shows better agreement with real data in 12 out of 16 time-windows. On average, SVR-CV exhibits a gain of approximately 8% in RMSE error compared to SVR. The study reveals that the cross-validation can result in a gain in RMS error as high as 33%, as observed in the time-window 14:30-14:45.
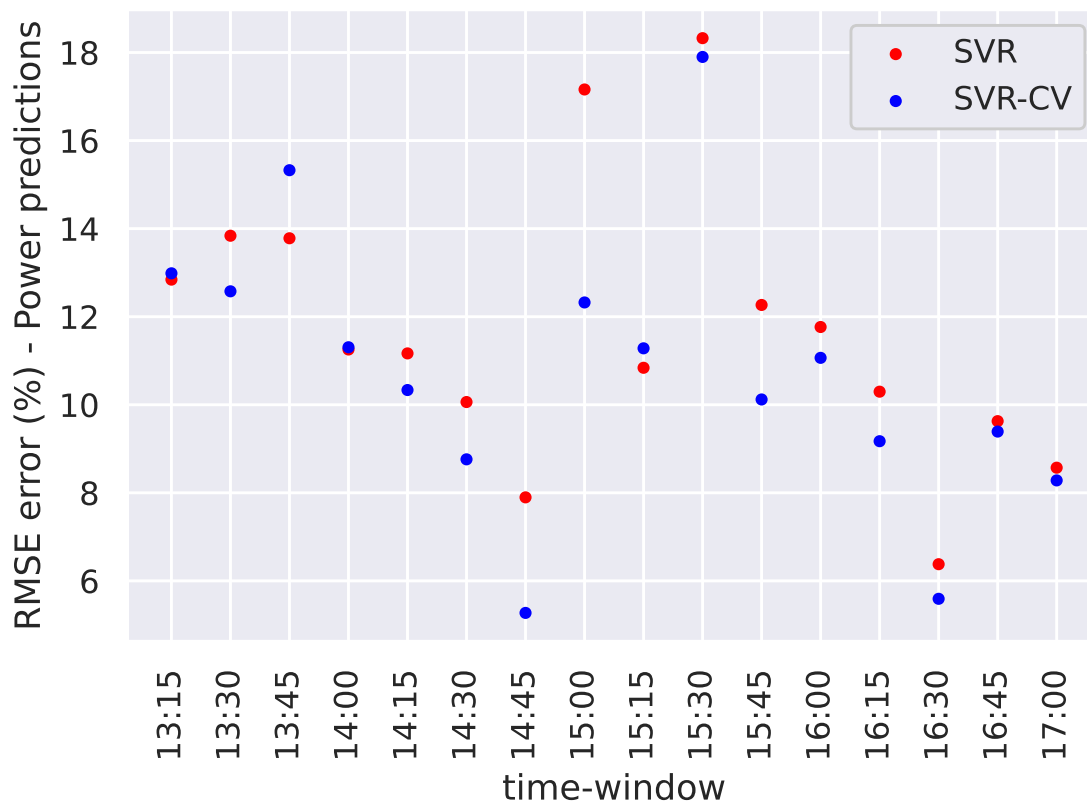
Figure 6. The power predictions error for the time-windows 13:00-13:15 to 16:45-17:00. 80% of the data have been used for the training and the rest of the data is used for the predictions that are compared with the real data. SVR compared to SVR-CV.

Table 3. The power predictions errors for the time between $13:00 - 17:00$. RMSE = root mean square error. SVR compared to SVR-CV.

			SVR compared to SVR-CV				
Window	Real data (mean value)	SVR prediction (mean value)	SVR-CV prediction (mean value)	SVR RMSE	SVR-CV RMSE	Difference in RMSE	Best parameters obtained by cross validation
13:00-13:15	436.6414	431.1161	462.0369	0.1284	0.1298	- 1.13 %	'C': 10, 'epsilon': 0.2, 'gamma': 0.01, 'kernel': 'rbf'
13:15-13:30	454.2678	437.7086	411.9456	0.1383	0.1257	+ 9.06 %	'C': 1, 'epsilon': 0.27, 'gamma': 0.1, 'kernel': 'rbf'
13:30-13:45	513.9758	450.5968	444.6124	0.1378	0.1532	- 11.22 %	'C': 10, 'epsilon': 0.2, 'gamma': 0.01, 'kernel': 'rbf'
13:45-14:00	466.5867	468.1083	467.04558	0.1125	0.1130	- 0.49 %	'C': 2, 'epsilon': 0.2, 'gamma': 0.1, 'kernel': 'rbf'
14:00-14:15	463.8826	495.3884	476.1067	0.1116	0.1033	+ 7.39 %	'C': 2, 'epsilon': 0.2, 'gamma': 0.01, 'kernel': 'rbf'
14:15-14:30	455.6234	539.7051	535.6208	0.1006	0.0876	+ 12.91 %	'C': 1, 'epsilon': 0.27, 'gamma': 0.01, 'kernel': 'rbf'
14:30-14:45	465.4522	517.7594	461.0503	0.0789	0.0527	+ 33.17 %	'C': 1, 'epsilon': 0.27, 'gamma': 0.01, 'kernel': 'rbf'
14:45-15:00	412.4164	624.0937	583.2256	0.1716	0.1232	+ 28.18 %	'C': 1, 'epsilon': 0.27, 'gamma': 0.01, 'kernel': 'rbf'
15:00-15:15	419.6866	508.4634	515.0853	0.1083	0.1128	- 4.17 %	'C': 1, 'epsilon': 0.27, 'gamma': 0.01, 'kernel': 'rbf'
15:15-15:30	420.9805	582.9539	572.4973	0.1832	0.1789	+ 2.29 %	'C': 1, 'epsilon': 0.27, 'gamma': 0.01, 'kernel': 'rbf'
15:30-15:45	424.9075	509.5947	470.3976	0.1226	0.1012	+ 17.45 %	'C': 1, 'epsilon': 0.2, 'gamma': 0.01, 'kernel': 'rbf'
15:45-16:00	454.6959	486.7116	478.8921	0.1176	0.1106	+ 5.90 %	'C': 1, 'epsilon': 0.27, 'gamma': 0.01, 'kernel': 'rbf'
16:00-16:15	479.6587	411.2667	494.2966	0.1029	0.0917	+ 10.86 %	'C': 100, 'epsilon': 0.27, 'gamma': 0.01, 'kernel': 'rbf'
16:15-16:30	447.9367	389.1476	436.7477	0.0637	0.0559	+ 12.19 %	'C': 1, 'epsilon': 0.27, 'gamma': 0.01, 'kernel': 'rbf'
16:30-16:45	491.8764	463.3234	465.1299	0.0962	0.0939	+ 2.38 %	'C': 1, 'epsilon': 0.27, 'gamma': 0.01, 'kernel': 'rbf'
16:45-17:00	488.9956	426.7180	461.8803	0.0857	0.0828	+ 3.36 %	'C': 1, 'epsilon': 0.2, 'gamma': 0.7, 'kernel': 'rbf'

5   Conclusions

The conclusions of this study highlight the benefits of employing an empirical mode decomposition (EMD)-based decoupling procedure as a preprocessor to support vector regression (SVR), and parameter tuning by using a cross-validation method for improving day-ahead wind power forecasting. In Sweden the intraday market works with 15-minute packages and with a 60-minute leading time. To fit this timeline, we used 15-minute averaged power data as our input for prediction. We divided the data set into 15-minute time-windows and calculated the average within each window. These averaged values were then used as input features for our forecasting model.

For making predictions, we used the power data from the previous four 15-minute time-windows as input and forecasted the power production for the 15-minute time-window that is 60 minutes ahead. This aligns with the timeline of the intraday market, where predictions need to be made with a 60-minute leading time to account for the operational requirements of the market.

In the first stage of the study, where SVR is compared to EMD-SVR, it is found that for five out of sixteen 15-minute time-windows, the IMF or IMF combinations obtained from EMD approximate the real data better than using pure SVR in the prediction process. The maximum error in approximating power productions with this method is 16%. Ten out of sixteen time-windows are predicted with an error of up to 11%, and four of those are predicted with an error of less than 10%. These results suggest that EMD-based signal decomposition can increase accuracy in wind power/speed forecasting.

In the second stage of the study, where cross-validation is applied (SVR-CV), better overall approximations are obtained compared to the SVR method (approximately +8% RMS error, averaged over 16 time-windows). Tuning the parameters of the SVR method using cross-validation shows a significant advantage compared to using preset parameter values. This indicates that parameter tuning can greatly improve the performance of SVR for wind power forecasting.

This study is tailored to the specific requirements of the intraday market and provides relevant insights for improving wind power forecasting within this timeline. Overall, the study suggests that employing an EMD-based decoupling procedure and applying cross-validation for parameter tuning can enhance the accuracy of wind power forecasting for the intraday market using SVR.

Competing interests.   The authors declare that none of the authors has any competing interests.

References

Vindbrukskollen, https://vbk.lansstyrelsen.se/en, accessed: 2022-07-19.

Abedi, H., Sarkar, S., and Johansson, H.: Numerical modelling of neutral atmospheric boundary layer flow through heterogeneous forest canopies in complex terrain (a case study of a Swedish wind farm), Renewable Energy, 180, 806–828, 2021.

Altıntaş, A. and Davidson, L.: EMD-SVR: a hybrid machine learning method to improve the forecasting accuracy of highway tollgates traveling time to improve the road safety, in: Intelligent Transport Systems, From Research and Development to the Market Uptake: 4th EAI International Conference, INTSYS 2020, Virtual Event, December 3, 2020, Proceedings 4, pp. 241–251, Springer, 2021.

Altıntaş, A., Davidson, L., and Peng, S.: A new approximation to modulation-effect analysis based on empirical mode decomposition, Physics of Fluids, 31, 025 117, 2019.

Altıntaş, A., Davidson, L., Kostaras, G., and Isaac, M.: The Day-Ahead Forecasting of the Passenger Occupancy in Public Transportation by Using Machine Learning, in: Intelligent Transport Systems, edited by Martins, A. L., Ferreira, J. C., and Kocian, A., pp. 3–12, Springer International Publishing, 2022.

Altıntaş, A., Davidson, L., and Carlson, O.: Forecasting of day-ahead wind speed/electric power by using a hybrid machine learning algorithm, in: Sustainable Energy for Smart Cities, edited by João L. Afonso, Vitor Monteiro, J. G. P., Springer International Publishing, 2023.

Hu, X., Jaraitė, J., and Kažukauskas, A.: The effects of wind power on electricity markets: A case study of the Swedish intraday market, Energy Economics, 96, 105 159, 2021.

Huang, C.-J. and Kuo, P.-H.: A Short-Term Wind Speed Forecasting Model by Using Artificial Neural Networks with Stochastic Optimization for Renewable Energy Systems, Energies, 11, 2018.

Huang, C.-M., Kuo, C.-J., and Huang, Y.-C.: Short-term wind power forecasting and uncertainty analysis using a hybrid intelligent method, IET Renewable Power Generation, 11, 678–687, 2017.

Huang, N. E., Shen, Z., Long, S. R., Wu, M. C., Shih, H. H., Zheng, Q., Yen, N.-C., Tung, C. C., and Liu, H. H.: The empirical mode decomposition and the Hilbert spectrum for nonlinear and non-stationary time series analysis, Proceedings of the Royal Society of London. Series A: mathematical, physical and engineering sciences, 454, 903–995, 1998.

Liu, Z., Hajiali, M., Torabi, A., Ahmadi, B., and Simoes, R.: Novel forecasting model based on improved wavelet transform, informative feature selection, and hybrid support vector machine on wind power forecasting, Journal of Ambient Intelligence and Humanized Computing, 9, 1919–1931, 2018.

Qiu, X., Suganthan, P. N., and Amaratunga, G. A.: Short-term electricity price forecasting with empirical mode decomposition based ensemble kernel machines, Procedia Computer Science, 108, 1308–1317, 2017.

Santamaría-Bonfil, G., Reyes-Ballesteros, A., and Gershenson, C.: Wind speed forecasting for wind farms: A method based on support vector regression, Renewable Energy, 85, 790–809, 2016.

Tan, L., Han, J., and Zhang, H.: Ultra-Short-Term Wind Power Prediction by Salp Swarm Algorithm-Based Optimizing Extreme Learning Machine, IEEE Access, 8, 44 470–44 484, 2020.

Würth, I., Valldecabres, L., Simon, E., Möhrlen, C., Uzunoğlu, B., Gilbert, C., Giebel, G., Schlipf, D., and Kaifel, A.: Minute-scale forecasting of wind power—results from the collaborative workshop of IEA Wind task 32 and 36, Energies, 12, 712, 2019.

Yang, J.: A novel wind power capacity combined forecasting method based on backtracking search algorithm, in: 2015 International Industrial Informatics and Computer Engineering Conference, pp. 720–723, Atlantis Press, 2015.

Zavala, A. J. and Messina, A. R.: Dynamic harmonic regression approach to wind power generation forecasting, in: 2016 IEEE PES
    Transmission & Distribution Conference and Exposition-Latin America (PES T&D-LA), pp. 1–6, IEEE, 2016.